Fractal models for the autocatalytic growth of amorphous thin films

Xiao-dan Pan, Andras Szasz,[a] and Derek J. Fabian
Scottish Surface and Materials Analysis Centre, Department of Physics and Applied Physics, University of Strathclyde, 48 North Portland Street, Glasgow G1 1XN, United Kingdom

(Received 6 September 1988; accepted for publication 8 February 1989)

Fractal models are proposed for the autocatalytic growth of amorphous thin films. The models give good agreement with the growth kinetics measured for electroless deposited films of amorphous nickel-phosphorus. A universal result obtained from the models is discussed, and only self-similarity is found to be important; randomness is effectively eliminated in the model.

INTRODUCTION

Electroless deposition is a useful technique for the preparation of amorphous (glassy) thin films and for studying their growth kinetics. The growth is slow, by contrast for example to superquenching, and it is relatively easy to follow and to investigate the buildup of the film. Moreover, many important physical and chemical processes are involved: nucleation, autocatalysis, metastable states, etc.,[1–5] and a study of the growth provides a valuable key to our understanding of these.

For a study of autocatalytic growth, we have chosen electroless deposited amorphous nickel-phosphorus (*a*:Ni-P) as a model system. This material is a typical binary metal-metalloid glass and has been widely investigated. Based on the results of experimental investigations, two fractal models are proposed to explain the growth kinetics.

EXPERIMENTAL OBSERVATIONS

From our reported measurements[1] of slow electroless deposition of *a*:Ni-P films, it was concluded that the growth has three stages: In stage I, a slow process of nucleation takes place, followed by a buildup of layers to a thickness of about 0.1 μm. The nucleation occurs at some sensitive points on the substrate, but the real growth starts only after the number of these points has reached a critical limit.[6] Because the amorphous state is known to require homogeneous and isotropic growth, the shape of the growing nuclei must be spherical. This is confirmed by microscopic examination.[1,2]

In stage II of the growth, which is a consequence of the globular (spherical) growth in stage I and of the whole surface of the initial globules being sensitive for new nucleation (autocatalysis), the growth network becomes three dimensional. Provided the growing hemispheres remain large, the deposition rate increases with increasing area of surface. During growth, gas bubbles—hydrogen, for example—are liberated freely from solution. Thus, when two growing spheres become close and are about to make contact, a gaseous interface is formed between them. This interface and the high surface tension in its region will prevent further nucleation. The growth is halted in such regions (a "self-stopping" behavior) and the spheres are prevented by the occluded gas from ultimately touching. Consequently the volume of space for the necessary isotropic growth becomes more and more limited, and the new spheres formed become smaller and smaller.

The final stage of growth, stage III, involves the formation of spheres so small that effectively a two-dimensional network of sensitive points is produced. The deposition rate becomes slower and finally the growth tends to saturate.

The three stages of growth can be clearly seen from the measured kinetics. Figure 1 shows the results obtained by monitoring the decrease in intensity of a given x-ray diffraction line of the substrate. Since the mass of the deposited film is proportional to its average thickness, the mass-versus-t curves will have the same shape as d-vs-t curves.

THE SIMPLE FRACTAL MODEL

Based on the experimental results, we propose a simple fractal model for the electroless growth of *a*:Ni-P thin films. Mathematically, the buildup by sequential spherical growth (Fig. 2) can be regarded as fractal.[7] Since the amorphous structure is homogeneous and isotropic, the fractal must be self-similar. We assume it to be a Cantor-block fractal[8] [Fig. 3(a)]; i.e., a hemispherical nucleation cluster is simplified to a regular block cluster.

Suppose in the first step of growth there are Q equivalent blocks nucleated on the substrate, whose area is A_0. In the second steps, the surface of each deposited block (area A_1) serves as a new substrate surface on which Q equivalent blocks are again deposited, and so on. If A_i is the area of such

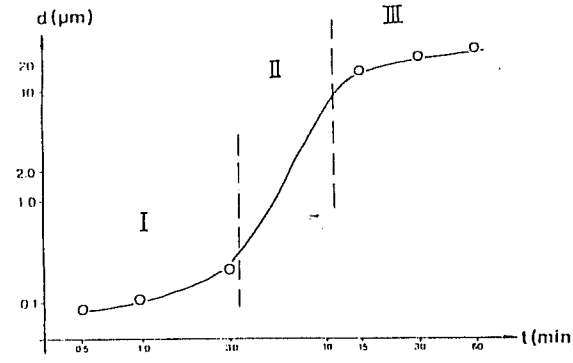

FIG. 1. The growth kinetics of *a*:Ni-P thin films by electroless deposition (see Ref. 1) showing three stages of growth. d is the average thickness of the growing film and t is the time of growth.

[a] Laboratory of Surface and Interface Physics, Eotvos University, Muzeum krt 6-8, Budapest, VIII, H1088, Hungary.

 0021-8979/89/130146-06$02.40

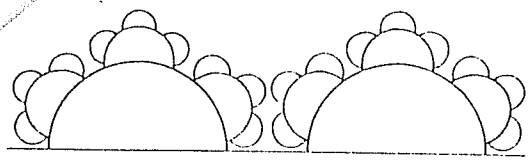

FIG. 2. A simulated sequential spherical fractal growth.

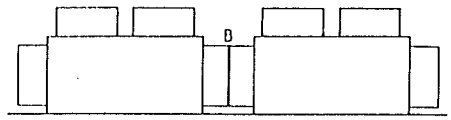

FIG. 4. The Cantor-block fractal with a three-dimensional growth. B is the point of "contact."

a substrate for the $(i+1)$th growth step, and $\xi_i = (A_i/Q - A_{i+1})$ is the surrounding empty area around each block deposited on A_i [shown in Fig. 3(b)], then

$$A_{i+1} = \frac{A_i}{Q} - \xi_i = \frac{A_i}{Q}\left(1 - \frac{Q\xi_i}{A_i}\right).$$

As the fractal is self-similar, $Q\xi_i/A_i = \xi$ should be constant, thus

$$A_{i+1} = (A_i/Q)(1-\xi) = A_0[(1-\xi)^{i+1}/Q^{i+1}]. \quad (1)$$

Suppose that in each growth step one layer of blocks is built up, then

$$M_k = \sum_{i=1}^{k} \rho_0 Q^i A_i b_i,$$

in which M_k is the total mass of deposited film after k layers are deposited, h_i is the height of the blocks that form the ith layer, and ρ_0 (a constant) is the density of the deposited film.

We assume $h_i = \alpha(A_i)^{1/2}$, where α is a shape factor defined by $\alpha = v(i)/(A_i)^{3/2}$, in which $v(i)$ is the volume of a block formed in the ith step of growth. For example, α is 1 for cubic blocks, and is $1/[3(2\pi)^{1/2}]$ for hemispheres. Then

$$M_k = \alpha\rho_0 A_0^{3/2} x[(1-x^k)/(1-x)], \quad (2)$$

in which $x = (1-\xi)^{3/2}/Q^{1/2}$.

Let us consider the growth shown in Fig. 4. We propose that nucleation and growth halt at points of "contact" such as B are approached (i.e., the self-stopping behavior already described). Mathematically, if there were not such points of contact, then for a total external area A_i' of a growing block at the ith step defined by $A_i' = \beta A_i$ in which β is a further shape factor ($\beta = 3$ for a semicube for example), we would have

$$A_{i+1} = A_i'[(1-\xi)/Q] = A_0[\beta^i(1-\xi)^{i+1}/Q^{i+1}], \quad (1')$$

and $v(i)$, the volume of each block formed in the ith step of growth, is given by

$$v(i) = A_i h_i = \alpha(A_0/\beta)^{3/2}[\beta^{3/2}(1-\xi)^{3/2}/Q^{3/2}]^i, \quad (3)$$

so that the total volume of the blocks grown in the ith step would be

$$V_i = Q^i v(i). \quad (4)$$

In practice, when points of "contact" do exist (in every step of the growth), we assume that their existence has an effect only on the value of V_i. We average the effect by defining a new parameter v_i^*, which represents the mean volume of a block grown at the ith step.

Thus we find (in reality), on introducing a factor

$$f_i = [v_i^*/v(i)] < 1,$$

where, for all $i > 0$, resulting from similarity, $f_{i+1} = f_i = f$, that

$$V_i = Q^i v_i^* = f Q^i v(i), \quad (4')$$

and we can write

$$M_k = \alpha f \rho_0 A_0^{3/2} x[(1-y^k)/(1-y)], \quad (2')$$

in which

$$y = \beta^{3/2} x.$$

Q is the number of (equivalent) blocks at the commencement of growth and, in the fractal model, remains constant during growth.

Since $Q \gg 1$, and $0 < \xi < 1$, $x \ll 1$. Thus, for semispherical blocks of radius R (Fig. 5) the surface area $A_i' = 2\pi R^2$. If a simulated block has a height $\sim R$, then for this block to have the same external surface area A_i', because $A_i \sim 4R^2$, $\beta = A_i'/A_i \sim \pi/2$. Thus in general we have $(\beta^{3/2}x) < 1$, i.e., $y < 1$.

Both Eqs. (2) and (2') can be written

$$M_k = c(1-a^k), \quad (5)$$

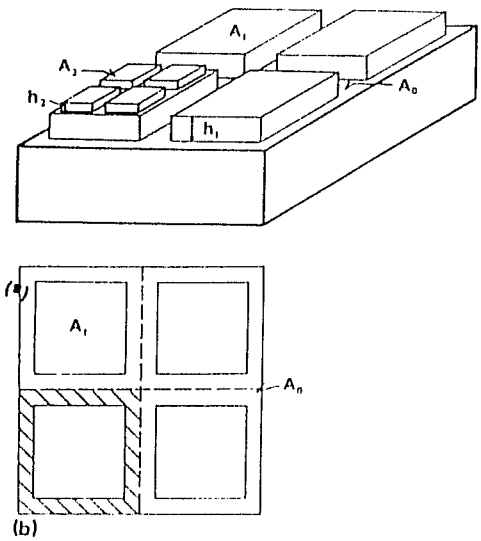

FIG. 3. (a) A Cantor-block fractal with $Q = 4$, where Q is the number of equivalent fractal blocks initially nucleating on the substrate. (b) The surrounding empty area of this fractal, dashed area is $\xi_{\quad 1}$, A_0 is the area of substrate, A_1, A_2 are the areas of the first- and second-step blocks, and h_1, h_2 are the heights of the first- and second-step blocks.

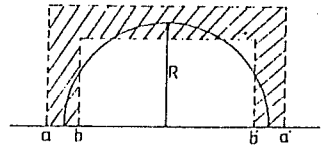

FIG. 5. Lateral cross section of the hemispherical block, in relation to the simulated block. R is the radius of the hemispherical block; the dashed area is the range in which the sizes of the simulated block can vary.

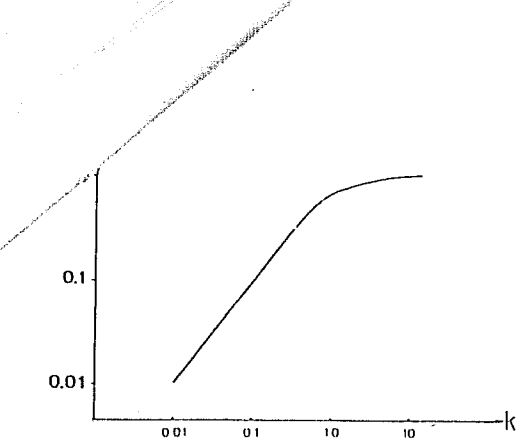

FIG. 6. Calculated kinetics, i.e., M_k vs k.

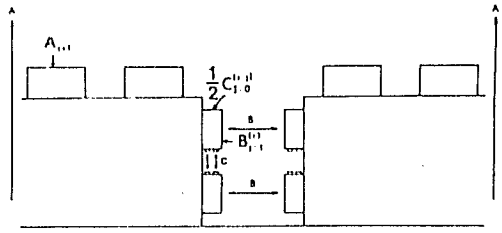

FIG. 7. Space limitation of the growth: A is the direction of growth vertical on a basic block of surface area A_i; no limit in vertical growth for area A_i. B is the parallel direction of growth of blocks grown on area $B_j^{(i)}$. C is the vertical direction of growth of the blocks grown on area $C_j^{(i,j)}$.

where a and c are constants, with $a < 1$. [$a = x$ in Eq. (2), and $a = y$ in Eq. (2').]

We find the curve of M_k vs k to have a general shape, shown in Fig. 6, and if we assume that $k = rt^l$ (where r and l are positive constants), then the M_k-vs-t curve will be similar, only compressed or extended linearly in the t direction (measured logarithmically—see Appendix A). We note agreement with the experimental curve (Fig. 1) except for the first stage, which is because fractal growth commences in the second stage.

On the other hand, it is necessary for self-similarity in our model that the first-step substrate of area A_0 should be the same as in the second, third, and subsequent steps, of areas A_i ($i > 0$). This requires that the entire area (A_0) of the substrate be covered by the deposited film before true fractal growth can begin. For example, in the electroless deposition of a:Ni-P, the substrate must be homogeneously covered by a very thin layer of a:Ni-P before the fractal growth commences.

The formation of this first monolayer requires surface nucleation and is nonfractal (stage I): It usually results in an incubation period before a homogeneous layer can be formed.[6] Growth of this monolayer only commences after the number of sensitive nucleation sites on the substrates has reached a given threshold.

THE RANDOM FRACTAL MODEL

We now consider a random fractal model, using the simple fractal model as a basis. A random growth process is assumed, in order to account for unknown random growth factors, but self-similarity is maintained. Thus, if we choose a growth parameter, for example, the thickness of the film deposited in the ith growth step t_i then the relation

$$t_{i+1} = \omega t_i,$$

with ω constant, remains valid for all steps. We still have a Cantor-block picture for the growth [Fig. 3(a)], but growth randomness is taken into account, resulting from surface inhomogeneity and from sites on the substrate (and subsequently the surface of growing blocks) being nonactive and therefore not completely covered by blocks as in the simple fractal model. The formation of nuclei, before the growth of blocks, can depend on several factors: e.g., gas bubbles, contamination, and surface defects

Growth occurs layer by layer, and overall is vertical to the substrate; i.e., in a direction perpendicular to the x-y plane (see A in Fig. 7). This therefore is the important direction in our model, and all parameters concerning this direction are given the subscript $\perp$.

As in the simple fractal model, we define $Q_\perp$ as the fractal magnification factor in the $\perp$ direction.[7] Initially there must be a substrate surface in, or parallel to, the x-y plane, with area A_0. In the first step, there would be at most $Q_\perp$ blocks forming on A_0, each with area A_1 (also parallel to the x-y plane). In our random model, there will be only $Q_\perp p_\perp$ blocks growing on A_0, where $p_\perp$ is the probability for "occupation." This leaves $Q_\perp (1 - p_\perp)$ sites on A_0 empty. In the second step of the vertical growth either each area A_1, or each empty site of A_0, serves as a new substrate where again only $Q_\perp p_\perp$ blocks can form.

$V_\perp^{(i)}$ is the volume of all the blocks formed in the ith layer, and if the height of each block is $h_i = \alpha(A_i)^{1/2}$, as before, with the shape factor $\alpha = v^{(i)}/(A_i)^{3/2}$, where $v^{(i)}$ = the volume of a simple block formed in the ith step, then

$$V_\perp^{(1)} = Q_\perp p_\perp \alpha A_0^{3/2}. \tag{6}$$

Remembering that in the simple fractal model, before randomness is introduced [Eq. (1')], $A_i \propto A_0(1 - \xi_\perp)^i/(Q_\perp)^i$, we can see that this expression remains valid, where $\xi_\perp$ is the percentage of the "empty" region of the substrate, and therefore

$$V_\perp^{(1)} = \alpha A_0^{3/2} p_\perp [(1 - \xi_\perp)^{3/2}/(Q_\perp)^{1/2}], \tag{6'}$$

giving, in the general case (see also Appendix B),

$$V_\perp^{(i)} = \alpha A_0^{3/2} [p_\perp (1 - \xi_\perp)^{3/2}/(Q_\perp)^{1/2}] y_\perp^{i-1}, \tag{7}$$

in which

$$y_\perp = [p_\perp (1 - \xi_\perp)^{3/2} + (1 - p_\perp)]/(Q_\perp)^{1/2};$$

clearly $y_\perp < 1$, since $0 < p_\perp \leq 1$, $0 < \xi_\perp < 1$, and $Q_\perp > 1$.

Now we can consider growth parallel to the x-y plane (see B in Figs. 7 and 8). This we also regard as one dimensional, because growth occurs equally for all directions parallel to the x-y plane. All parameters concerning this direction are given the subscript $\parallel$. Let the fractal magnification in this direction be $Q_\parallel$, and the probability for occupation be $p_\parallel$. Then if $V_\parallel^{(i,j)}$ is the volume of all the blocks formed in the jth step of parallel growth (blocks that originate from the blocks formed in the ith step of vertical growth) and if we assume that the height of these blocks $h_j^{(i)} = \gamma[B_j^{(i)}]^{1/2}$ (where γ is a shape factor in the $\parallel$ direction, corresponding to α in the $\perp$ direction), with $B_0^{(i)} = \mu A_i$ (where μ is a

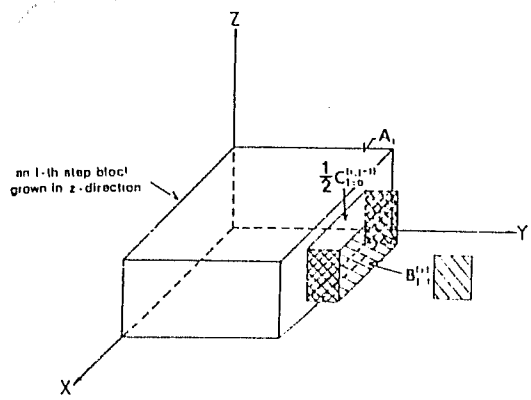

FIG. 8. Growth parallel to the x-y plane. The larger block is an ith step block, grown in the z direction with a top face of area A_i and total external area A_i. The dashed area is $B_{i-1}^{(i)}$. Dashed plus hatched areas is $B_j^{(i)}$.

further shape factor; e.g., μ is 4 for cubic blocks, see Appendix C), then for $i = 1$,

$$V_{\parallel}^{(ij)} = Q_1 p_\perp \gamma (\mu A_1)^{3/2} \frac{p_\parallel (1-\xi_\parallel)^{3/2}}{(Q_\parallel)^{1/2}} y_\parallel^{j-1}$$

$$= \gamma \mu^{3/2} A_0^{3/2} \frac{p_\perp (1-\xi_\perp)^{3/2}}{(Q_\perp)^{1/2}} \frac{p_\parallel (1-\xi_\parallel)^{3/2}}{(Q_\parallel)^{1/2}} y_\parallel^{j-1}, \quad (8)$$

in which

$$y_\parallel = [1/(Q_\parallel)^{1/2}][p_\parallel \eta^{3/2}(1-\xi_\parallel)^{1/2} + (1-p_\parallel)],$$

where η is a further shape factor (Appendix C), and $\xi_\parallel$ is the percentage of empty area on the substrate for the $\parallel$ direction of growth (when randomness is not considered). In Appendix C we illustrate why $y_\parallel < 1$. Finally we find

$$V_{\parallel}^{(ij)} = \gamma \mu^{3/2} A_0^{3/2} p_\perp \frac{(1-\xi_\perp)^{3/2}}{(Q_\perp)^{1/2}} y_\perp^{i-1} p_\parallel \frac{(1-\xi_\parallel)^{3/2}}{(Q_\parallel)^{1/2}} y_\parallel^{j-1}, \quad (9)$$

and, if $V(k)$ is the total volume of blocks for the initial k "layers," we have as a first approximation,

$$V(k) = \sum_{i=1}^{k} (V_\perp^{(i)} + V_{\parallel}^{(ij)})$$

$$= A_0^{3/2} p_\perp \frac{(1-\xi_\perp)^{3/2}}{(Q_\perp)^{1/2}} \theta(j) \sum_{i=1}^{k} y_\perp^{i-1} \quad (10)$$

$$\theta(j) = \alpha + \gamma \mu^{3/2} \left(\frac{p_\parallel (1-\xi_\parallel)^{3/2}}{(Q_\parallel)^{1/2}} \right) \sum_j y_\parallel^{j-1}.$$

The Σ_j covers all possible values for j for $i \leqslant k$.

In the second approximation, the growth originating from $C_I^{(ij)}$ surfaces parallel to the x-y plane (Fig. 8) is taken into account.

Suppose $C_0^{(ij)} = \epsilon B_j^{(i)}$, with $\epsilon =$ shape factor like μ, then

$$V(k) = A_0^{3/2} \frac{p_\perp (1-\xi_\perp)^{3/2}}{(Q_\perp)^{1/2}} \left[\alpha + \frac{\theta(j)-\alpha}{\gamma} (\gamma + \alpha \epsilon^{3/2} \times \frac{p_\perp (1-\xi_\perp)^{3/2}}{(Q_\perp)^{1/2}} \sum_I y_\perp^{I-1} \right) \Bigg] \sum_{i=1}^{k} y_\perp^{i-1}. \quad (11)$$

In the third approximation, the growth originating from the surfaces (those vertical to the x-y plane and those belonging to the blocks grown on $C_I^{(ij)}$ surfaces) is taken into account. We find similarly

$$V(k) = A_0^{3/2} \frac{p_\perp (1-\xi_\perp)^{3/2}}{(Q_\perp)^{1/2}} \left[\alpha + \frac{\theta(j)-\alpha}{\gamma} \left(\gamma + \epsilon^{3/2} \times \frac{p_\perp (1-\xi_\perp)^{3/2}}{(Q_\perp)^{1/2}} \theta(m) \sum_I y_\perp^{I-1} \right) \right] \sum_{i=1}^{k} y_\perp^{i-1}. \quad (12)$$

We see in Fig. 7 that the space for growth on $C_I^{(ij)}$ is much more limited than for growth on $B_j^{(i)}$, while this growth is also severely limited in comparison with the growth on A_i. Noting the self-stopping behavior of growth we can assume that for $i \lesssim k$, the possible values for $j, I, m, \ldots$, etc., go to infinity. This assumption is acceptable because as the space for growth becomes limited, the growing blocks become very small, and the range of summation affects the result by very little. Equation (12) then becomes

$$V(k) = A_0^{3/2} \frac{p_\perp (1-\xi_\perp)^{3/2}}{(Q_\perp)^{1/2}} \left[\alpha + \frac{\theta(j)-\alpha}{\gamma} \left(\gamma + \epsilon^{3/2} \times \frac{p_\perp (1-\xi_\perp)^{3/2}}{(Q_\perp)^{1/2}} \frac{V(\infty)}{A_0^{3/2} p_\perp (1-\xi_\perp)^{3/2} (Q_\perp)^{-1/2}} \right) \right] \times \sum_{i=1}^{k} y_\perp^{i-1}. \quad (12')$$

When $k \to \infty$, $v(\infty)$ can be found by solving (12'). $V(\infty)$ is a constant. Lastly, (12') can be written

$$V(k) = D[(1-y_\perp^k)/(1-y_\perp)], \quad (13)$$

and

$$M_k = \rho_0 V(k) = \rho_0 D(1-y_\perp^k)/(1-y_\perp), \quad (13')$$

where D is a function of $A_0, p_\perp, p_\parallel, Q_\perp, Q_\parallel, \xi_\perp, \xi_\parallel, \alpha, \gamma, \mu, \epsilon$, and η which can all be regarded as constants.

In the simplest case, we assume $p_\perp = p_\parallel = p$, and the self-similarity is conserved in three dimensions: $Q_\perp = Q_\parallel = Q$, $\xi_\perp = \xi_\parallel = \xi$, and $\alpha = \gamma$.

Also, if $A_i' = \beta A_i$, as shown by Fig. 4, then (1') is still valid. Following the process used to derive (7), we find

$$V^{(i)} = \alpha A_0^{3/2} [p(1-\xi)/Q^{1/2}] Y^{i-1},$$

in which

$$Y = [p\beta^{3/2}(1-\xi) + (1-p)]/Q^{1/2},$$

and then

$$M_k = \rho_0 \sum_{i=1}^{k} V^{(i)} = \alpha \rho_0 A_0^{3/2} \frac{p(1-\xi)^{3/2}}{Q^{1/2}} \frac{1-y^k}{1-y}. \quad (14)$$

This is the random case of the growth shown in Fig. 4. Note both Eqs. (13') and (14) have the same form as (5).

DISCUSSION

Despite randomness, our fractal model gives the same growth kinetics. Both models agree well with the measured kinetics except in the first stage of growth, where a process of slow nucleation occurs that can be simulated by a two-dimensional growth. In our view, although the fractal growth actually starts during the second stage, it determines the mode of growth in the first stage, because to ensure fractal

similarity it is necessary that the substrate for the first stage of fractal growth be the same as becomes available for the second, third, and subsequent stages. This is why the substrate must first be covered by a deposited layer. Thus, first there is an incubation time, during which the substrate becomes homogeneously covered by a very thin layer; and second, as soon as the substrate is covered, the fractal growth and no other growth, occurs. This continues until the space limitation causes onset of stage three, which gives rise again to a two-dimensional surface that is only stable[9,10] as long as local inhomogeneities do not cause a further fractal growth.

The universal property displayed by the two fractal models is the result of the self-similarity. Because of self-similarity the growth does not depend strongly on the specific chemical nature of the growth process and, regardless of inhomogeneity of the actual shape of growing units (blocks), the growth kinetics and the structure of the film will always be of the same form. We believe that these models will remain valid in general for the autocatalytic growth of amorphous films; the governing factor being always the self-similarity, which can thus be regarded also as the scaling in the growth.

CONCLUSION

We have proposed two mathematical models for the autocatalytic growth of amorphous thin films. They explain well the growth kinetics measured for electroless deposited *a*:Ni-P films. The importance of self-similarity in growth units has been demonstrated by the universal result obtained in our models.

APPENDIX A

Say we define $Y = \ln M$, $X = \ln k$, and a new $X' = \ln t$. Then dY/dX will have the same shape as dY/dX', if $K = \delta t^n$. This we can show as follows:

$$\frac{dY}{dX} = \frac{dY}{dM}\frac{dM}{dk}\frac{1}{dX/dk} = \frac{k}{M}\frac{dM}{dk} \tag{A1}$$

and

$$\frac{dY}{dX'} = \frac{t}{M}\frac{dM}{dt}. \tag{A2}$$

Suppose $k = \delta t^n$, with δ and n constant (not necessarily integers), and substitute in (1),

$$\frac{dY}{dX} = \frac{\delta t^n}{M}\frac{1}{dk/dt}\frac{dM}{dt} = \frac{1}{n}\frac{t}{M}\frac{dM}{dt} = \frac{1}{n}\frac{dY}{dX'},$$

from which we conclude that the M_k-vs-k curve, in logarithm axes (Fig. 6), will have the same general shape as an M_k-vs-t curve in logarithm axes [compressed by a factor of $(1/n)$].

Thus the agreement shown by Figs. 1 and 6 indicates that $k - \delta t^n$ is satisfied in the growth.

APPENDIX B

In the first step of deposition there are Q_1 sites for growth, on area A_0, and $Q_1 p_1$ blocks that form, each with growing upper area A_1 (parallel to A_0). There remain $Q_1(1-p_1)$ sites on A_0 emtpy, each of area A_0/Q_1. In the second step, each of $Q_1 p_1$ areas A_1 and every empty site of A_0 is available substrate—on which $p_1 Q_1$ blocks can form. Thus the total volume of blocks found in the second step of growth is

$$V_1^{(2)} = Q_1 p_1 v_2(A_1) + Q_1(1-p_1) V_2^{A_0}(\text{empty}),$$

where $v_2(A_1)$ is the volume of the block growing on each A_1 in this step, and $V_2^{A_0}(\text{empty})$ is the volume of the block growing on each empty site of A_0.

Clearly, for the second step of growth,

$$v_2(A_1) = Q_1 p_1\, \alpha\{[A_0/(Q_1)^2](1-\xi_1)^2\}^{3/2}$$

and

$$v_2^{A_0}(\text{empty}) = Q_1 p_1\, \alpha\{(A_0/Q_1)[(1-\xi_1)/Q_1]\}^{3/2},$$

so that

$$V_1^{(2)} = \alpha A_0^{3/2}\frac{p_1(1-\xi_1)^{3/2}}{(Q_1)^{1/2}}\left(\frac{p_1(1-\xi_1)^{3/2}+(1-p_1)}{(Q_1)^{1/2}}\right).$$

We define $A_2^{A_1}$ as the area of each block formed in the second step on A_1 (parallel to surface A_0), and $A_2^{A_0}$ as the area of each block formed in the second step on A_0, then

$$V_1^{(3)} = (Q_1 p_1)^2 v_3(A_2^{A_1}) + Q_1 p_1\, Q_1(1-p_1) \times v_3^{A_1}(\text{empty}) + Q_1(1-p_1)\, Q_1 p_1\, v_3(A_2^{A_0}) + [Q_1(1-p_1)]^2 v_3^{A_0}(\text{empty}).$$

Now, if $v_3(A_2^{A_1})$ and $v_3(A_2^{A_0})$ are the volumes of the blocks growing, respectively, on each $A_2^{A_1}$ and $A_2^{A_0}$ in the third step; and $v_3^{A_1}(\text{empty})$ and $v_3^{A_0}(\text{empty})$ are the volumes of the blocks forming on each empty site of A_1 and A_0 in the third step, respectively, then

$$v_3(A_2^{A_1}) = Q_1 p_1\, \alpha\{[A_0/(Q_1)^3](1-\xi_1)^3\}^{3/2},$$

$$v_3(A_2^{A_0}) = Q_1 p_1\, \alpha\{(A_0/Q_1)[(1-\xi_1)^2/(Q_1)^2]\}^{3/2},$$

$$v_3^{A_1}(\text{empty}) = Q_1 p_1\, \alpha\left(\frac{A_0}{Q_1}(1-\xi_1)\frac{1}{Q_1}\frac{(1-\xi_1)}{Q_1}\right)^{3/2},$$

and

$$v_3^{A_0}(\text{empty}) = Q_1 p_1\, \alpha\{(A_0/Q_1)[(1-\xi_1)/Q_1]\}^{3/2}.$$

Thus

$$v_1^{(3)} = \alpha A_0^{3/2}\frac{p_1(1-\xi_1)^{3/2}}{(Q_1)^{1/2}}\left(\frac{p_1(1-\xi_1)^{3/2}+(1-p_1)}{(Q_1)^{1/2}}\right)^2$$

Giving, in general,

$$V_1^{(i)} = \alpha A_0^{3/2}\frac{p_1(1-\xi_1)^{3/2}}{(Q_1)^{1/2}} \times \left(\frac{p_1(1-\xi_1)^{3/2}+(1-p_1)}{(Q_1)^{1/2}}\right)^{i-1}.$$

APPENDIX C

We show the parallel growth in Fig. 8. $B_0^{(i)}$ is defined as $(A_i' - A_i)$ and thus can be written as $B_0^{(i)} = \mu A_i$, $\mu = a$ shape factor. If we assume $B_{j=1}^{(i)\prime} = \eta B_{j=1}^{(i)}$ (where η = another shape factor) then, because of self-similarity, we have $B_j^{(i)\prime} = \eta B_j^{(i)}$ for all j. For the reason shown in Fig. 5, we know that $y_\parallel < 1$ is generally satisfied.

[1]A. Szasz, J. Kojnok, L. Kertesz, and Z. Hegedus, J. Non-Cryst. Solids 57, 213 (1983).
[2]A. Szasz, J. Kojnok, L. Kertesz, and Z. Hegedus, Thin Solid Films 116, 279, (1984).
[3]V. S. Demidenko, A. Szasz, and M. A. Aysawi, Phys. Status Solidi B 140, 121 (1987).
[4]A. Szasz, D. J. Fabian, Z. Paal, and J. Kojnok, J. Non-Cryst. Solids 103, 21 (1988).
[5]A. Szasz, X.-D. Pan, J. Kojnok, and D. J. Fabian, J. Non-Cryst. Solids 108, 304 (1989).
[6]J. Loranth, A. Szasz, and F. Schuszter, Plating Surf. Finish. 116 (May 1987).
[7]B. B. Mandelbrot, in *The Fractal Geometry of Nature* (Freeman, San Francisco, 1982).
[8]T. Kaplan, L. J. Gray, and S. H. Liu, Phys. Rev. B 35, 5379 (1987).
[9]W. W. Mullins and R. F. Skereka, J. Appl. Phys. 35, 444 (1964).
[10]A. Okamoto, J. Lagowski, and H. C. Gatos, J. Appl. Phys. 53, 1706 (1982).